Modulation of Phospholipid Acyl Chain Order by Cholesterol. A Solid-State ^2H Nuclear Magnetic Resonance Study†

Mantripragada B. Sankaram* and Thomas E. Thompson
Department of Biochemistry, University of Virginia Health Sciences Center, Charlottesville, Virginia 22908
Received June 8, 1990; Revised Manuscript Received August 22, 1990

ABSTRACT: The effect of cholesterol on the acyl chain order of three glycerophosphocholines with 14, 16, and 18 carbons per acyl chain, namely, di(14:0)PC, di(16:0)PC, and di(18:0)PC, above the gel to liquid-crystalline phase transition temperature was investigated by using ^2H nuclear magnetic resonance spectroscopy. Average acyl chain lengths were calculated from the segmental order parameters (S_{mol}) for the *sn*-1 and the *sn*-2 chains in the absence of cholesterol and at 3:1, 2:1, and 1:1 mole ratios of phospholipid–cholesterol. The three binary mixtures of cholesterol with phosphatidylcholines are in the liquid-ordered (l_o) phase. For all the three phosphatidylcholine–cholesterol systems, the distance from the carbonyl groups to the terminal methyl groups is shorter than the length of the cholesterol molecule. A molecular model for the l_o phase consistent with these observations has in a statistical sense a part of each cholesterol molecule in one monolayer extending into the other monolayer. This results in a packing arrangement akin to that in interdigitated systems. On the basis of the effect of cholesterol on phospholipid acyl chain orientational order, it is suggested that the liquid-disordered (l_d) phase at low cholesterol concentrations corresponds to a packing mode in which the cholesterol molecule spans the entire transbilayer hydrophobic region. A molecular mechanism is proposed in which increasing the concentration of cholesterol has the effect of stretching the acyl chains of phospholipids by increasing the population of trans conformers up to a stage where the hydrophobic length is considerably longer than the cholesterol molecule. Beyond this concentration, the partially interdigitated phase forms. This interpretation provides a molecular basis for the liquid-crystalline phase immiscibility in cholesterol-containing bilayers where the partially interdigitated phase corresponds to the liquid-ordered phase (l_o) and the noninterdigitated phase corresponds to the liquid-disordered (l_d) phase. It is suggested that the fluid phase immiscibility exhibited by cholesterol-containing lipid bilayers follows as a natural consequence of the length mismatch between the essentially rigid steroid and the flexible phospholipid acyl chains and that there is no need to invoke complex formation between the two components of this binary system.

Cholesterol is a ubiquitous component of eukaryotic cell membranes (Rouser et al., 1968). The cholesterol content of membranes is dependent on membrane composition (Rouser et al., 1968) and cellular growth and development (Boesze-Battaglia et al., 1989) and can be as high as 50 mol %. Physicochemical studies aimed at establishing a structure–function relation for cholesterol have suggested a cholesterol-concentration-dependent modulation of membrane fluidity (Huang, 1977; Yeagle, 1985, 1988) as a mechanism for regulating the activity of other membrane-associated components (Cooper, 1977).

Studies that showed abrupt changes at a critical cholesterol concentration in various physical parameters of the membrane have been interpreted in terms of formation of combinations of equimolar, 2:1, 3:1, and 4:1 phospholipid–cholesterol complexes or formation of ordered microscopic domains of solid and fluid (Lecuyer & Dervichian, 1969; Engelman & Rothman, 1972; Hinz & Sturtevant, 1972; Shimshick & McConnell, 1973; Phillips & Finer, 1974; Kleemann & McConnell, 1976; Opella et al., 1976; Estep et al., 1978; Mabrey et al., 1978; Copeland & McConnell, 1980; Lentz et al., 1980; Melchior et al., 1980; Snyder & Freire, 1980; Recktenwald & McConnell, 1981; Presti & Chan, 1982). This viewpoint has been successful in quantitatively analyzing heat capacity data (Snyder & Freire, 1980) on cholesterol-containing phospholipid bilayers. An alternative interpretation has been proposed that does not require specific stoichiometric phospholipid–cholesterol complex formation (Ipsen et al., 1987). In this model, the phospholipid–cholesterol mixture is treated as a pseudoternary system where the three components are chain-disordered phospholipid, chain-ordered phospholipid, and cholesterol. Assuming very different pairwise interaction energies between the three types of molecules, the gross features of the phospholipid–cholesterol phase diagrams can be reproduced reasonably well with this model (Sperotto et al., 1989).

Electron spin resonance (ESR)[1] and nuclear magnetic resonance (NMR) studies have indicated that the incorporation of increasing amounts of cholesterol into lipid bilayers in the liquid-crystalline phase is accompanied by an increase in the trans-conformer population for the individual acyl chain carbon–carbon linkages (Haberkorn et al., 1977; Oldfield et al., 1978; Stockton & Smith, 1976; Vist & Davis, 1990). However, at temperatures above the main transition tem-

† This research was supported by a grant from the National Institutes of Health (GM-14628).

[1] Abbreviations: (14:0)(per-^2H-14:0)PC, 1-myristoyl-2-(perdeuteriomyristoyl)-*sn*-glycero-3-phosphocholine; di(per-^2H-14:0)PC, 1,2-bis(perdeuteriomyristoyl)-*sn*-glycero-3-phosphocholine; (16:0)(per-^2H-16:0)PC, 1-palmitoyl-2-(perdeuteriopalmitoyl)-*sn*-glycero-3-phosphocholine; di(per-^2H-16:0)PC, 1,2-bis(perdeuteriopalmitoyl)-*sn*-glycero-3-phosphocholine; (18:0)(per-^2H-18:0)PC, 1-stearoyl-2-(perdeuteriostearoyl)-*sn*-glycero-3-phosphocholine; di(per-^2H-18:0)PC, 1,2-bis(perdeuteriostearoyl)-*sn*-glycero-3-phosphocholine; di(14:0)PC, 1,2-dimyristoyl-*sn*-glycero-3-phosphocholine; di(16:0)PC, 1,2-dipalmitoyl-*sn*-glycero-3-phosphocholine; di(18:0)PC, 1,2-distearoyl-*sn*-glycero-3-phosphocholine; ESR, electron spin resonance; NMR, nuclear magnetic resonance.

0006-2960/90/0429-10676$02.50/0

perature of the pure phospholipid and in the cholesterol concentration range 0–50 mol %, the chains never adopt the all-trans configuration. As the lipid acyl chain length is varied, the trans-conformer population and hence the bilayer thickness must be optimized so as to accommodate a given constant number of the essentially nonflexible cholesterol molecules in the lipid bilayer.

The phase diagrams for binary mixtures of cholesterol with glycerophospholipids (Shimshick & McConnell, 1973; Recktenwald & McConnell, 1981; Ipsen et al., 1987; Vist & Davis, 1990; Sankaram & Thompson, 1990) describe the phenomenon of fluid-phase immiscibility induced by cholesterol. Calorimetric (Vist & Davis, 1990) and spin-label electron spin resonance spectroscopic studies (Shimshick & McConnell, 1973; Sankaram & Thompson, 1990) on phosphatidylcholine–cholesterol mixtures have identified a liquid-disordered (l_d) phase in the cholesterol concentration range 0 to 7–23 mol %. A liquid-ordered (l_o) phase has also been identified in the concentration range 25–33 to 50 mol %. At intermediate cholesterol concentrations below a critical temperature, both the l_d and the l_o phases are presumed to coexist.

The intermolecular interactions between the flexible phospholipid molecules and the rigid cholesterol molecules must in some way modulate the phase behavior of the system. The l_o phase is of special interest in this regard since it may be the phase characteristic of biological membranes containing large amounts of cholesterol. For instance, human erythrocyte ghosts and *Acholeplasma laidlawii* grown on cholesterol-rich media have been suggested to be in a relatively fluid state, the spectral characteristics of which resemble those of the l_o state (Davis et al., 1980; Rance et al., 1982).

We examine here the l_o phase in detail by ^{2}H NMR in binary mixtures of cholesterol using three chain-perdeuterated glycerophosphocholines with increasing number of acyl chain carbons, namely, di(14:0)PC, di(16:0)PC, and di(18:0)PC. This method provides a direct determination of the degree of orientational averaging. The results of these studies, when used together with specific models for various possible packing arrangements of cholesterol with phospholipids, lead us to propose statistical arrangements for the molecules in the l_d and l_o phases.

Materials and Methods

Materials. Lysophosphatidylcholines were obtained from Avanti Polar Lipids (Birmingham, AL). The $CdCl_2$ complex of glycerophosphocholine was purchased from Sigma Chemical Co. (St. Louis, MO). Deuterium-depleted water was from Aldrich Chemical Co. (Milwaukee, WI). Perdeuterated myristic (14:0), palmitic (16:0), and stearic (18:0) acids were purchased from Cambridge Isotope Laboratories (Woburn, MA). Cholesterol was obtained from Nu-Chek-Prep (Elisian, MN).

(14:0)(per-^{2}H-14:0)PC, (16:0)(per-^{2}H-16:0)PC, and (18:0)(per-^{2}H-18:0)PC containing perdeuterated *sn*-2 chains were synthesized by acylating the corresponding lysophosphatidylcholines with perdeuterated carboxylic acid anhydrides (Mason et al., 1981). The diacylphosphatidylcholines with perdeuterated *sn*-1 and *sn*-2 chains, namely, di(per-^{2}H-14:0)PC, di(per-^{2}H-16:0)PC, and di(per-^{2}H-18:0)PC, were either purchased from Avanti Polar Lipids Inc. or chemically synthesized by reacting *sn*-glycero-3-phosphocholine with perdeuterated carboxylic acids in the presence of dicyclohexylcarbodiimide and 4-pyrrolidinopyridine. All the lipids were stored as lyophilized powders at −20 °C under nitrogen.

Sample Preparation. Multilamellar vesicles were prepared by dispersing in deuterium-depleted water about 20 mg of dry and thin films of the phospholipid–cholesterol mixtures obtained by evaporation of a $CHCl_3$–CH_3OH (2:1 v/v) solution containing required amounts of the lipid components. Complete hydration of the phospholipid–cholesterol mixtures was ensured during the process of lipid dispersal by thorough vortex mixing at approximately 10 °C above the gel to liquid-crystalline phase transition temperatures. The lipid dispersion was transferred to 5-mm-diameter glass tubes and concentrated by centrifugation in a bench centrifuge.

NMR Spectroscopy. NMR spectra were run on a Nicolet NT-360 spectrometer running at 45 MHz for the ^{2}H nucleus. A fixed-frequency high-power variable-temperature probe, HP-50 from Cryomagnet Systems, Inc. (Indianapolis, IN), with a 5-mm solenoid was used for the solid-state ^{2}H NMR experiments. The sample temperature was controlled by a Nicolet variable-temperature accessory. The quadrupole echo pulse sequence (Davis et al., 1976; Bloom et al., 1980) was used with a 90° pulse width of 2.4 μs. The interpulse delay was optimized for each sample to obtain a digitized point at the top of a symmetric echo and to minimize the imaginary part of the magnetization. The delay values were generally between 30 and 60 μs. A relaxation delay of 300 ms was used.

Data Analysis. The Fourier-transformed ^{2}H NMR spectra were transferred for further data processing from the Nicolet 1290 computer to an IBM 3090 mainframe computer via a Sun Microsystems workstation. The powder patterns were deconvoluted by using both the iterative (Bloom et al., 1981; Sternin et al., 1983) and noniterative (Whittall et al., 1989) de-Pakeing algorithms, using the software kindly provided by Drs. Myer Bloom, Edward Sternin, and Kenneth Whittall, which was modified to run on an IBM 3090 mainframe computer by using its vector processing capabilities.

The order parameter of the C–^{2}H bond, S_{C-D}, was calculated from the experimental residual quadrupole splittings, $\Delta\nu_Q$, according to the equation (Seelig & Seelig, 1974)

$$\Delta\nu_Q = \tfrac{3}{4}(e^2qQ/h)P_2(\cos\theta)S_{CD} \quad (1)$$

where $P_2(\cos\theta)$ is the second-order Legendre polynomial. The deuteron quadrupole splitting constant, e^2qQ/h, was taken to be 170 kHz, which is the value for most C–^{2}H bonds (Burnett & Muller, 1971). The segmental order parameter, S_{mol}, was calculated by using the equation

$$S_{mol} = |-2S_{CD}| \quad (2)$$

for methylene groups (Seelig & Seelig, 1974). The following equation was used to calculate the segmental order parameter for methyl groups (Stockton et al., 1976):

$$S_{mol} = |-6S_{CD}| \quad (3)$$

Results

^{2}H NMR Powder Patterns for di(per-^{2}H-14:0)PC and (14:0)(per-^{2}H-14:0)PC. Figure 1 shows ^{2}H NMR spectra of aqueous dispersions of di(per-^{2}H-14:0)PC with (Figure 1B) and without (Figure 1A) 50 mol % cholesterol in the liquid-crystalline phase at 35 °C. The experimental ^{2}H NMR spectra are seen in each case to consist of a series of overlapping powder patterns arising from the 13 inequivalent deuterated segments per chain (Davis, 1979). The sharp peaks correspond to the 90° orientation of the bilayer normal relative to the external magnetic field direction, and the shoulders in the wings with less intensity represent the 0° orientation (Seelig, 1977; Seelig & Seelig, 1980; Davis, 1983). The observed ^{2}H NMR line shapes are indicative of a random bilayer distribution (Davis, 1983).

The experimental powder-type ^{2}H spectra were deconvoluted, using both the iterative (Bloom et al., 1981; Sternin et

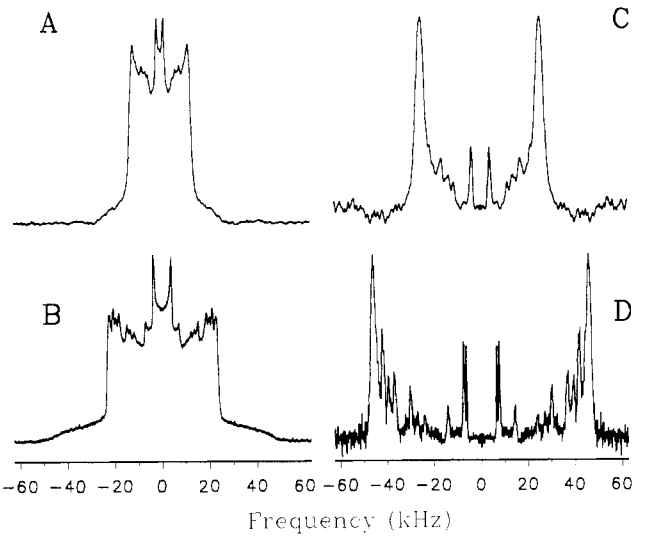

FIGURE 1: 45-MHz ^2H NMR spectra from aqueous dispersions of di(per-^2H-14:0)PC alone (A) and an equimolar mixture of cholesterol with di(per-^2H-14:0)PC (B) at 35 °C, corresponding to a reduced temperature of 0.041. The de-Paked spectra derived from (A) and (B) are shown in (C) and (D), respectively.

al., 1983) and the noniterative (Whittall et al., 1989) algorithms, to obtain the 0° orientation spectra assuming that the quadrupole splittings scale with the bilayer orientation θ as $(3\cos^2\theta - 1)$. The degree of spectral resolution obtained by both the algorithms was found to be the same for all the systems investigated here. The de-Paked spectra of the phospholipid alone and of the equimolar mixture obtained by the iterative de-Pakeing procedure are shown in parts C and D of Figure 1, respectively. The de-Pakeing algorithm, as is evident in Figure 1C,D, improves the spectral resolution by eliminating the powder part of the Pake doublet and thereby spreading out the spectrum to the maximum possible extent.

The sharp Pake-doublet with the smallest quadrupole splitting in the ^2H NMR spectra for aqueous dispersions of di(per-^2H-14:0)PC (Figure 1A,C) arises from the terminal C^2H_3 deuterons from both the *sn*-1 and the *sn*-2 chains. The two methyl groups are chemically and magnetically equivalent and have the same average orientations, which leads to a single doublet arising from both of them. However, addition of 50 mol % cholesterol leads to an inequivalence of the two methyl group deuterons (Figure 1B,D), thereby giving rise to two sharp Pake-doublets. The inequivalence of the terminal methyl groups is also found in the 3:1 and 2:1 di(per-^2H-14:0)PC–cholesterol (mol/mol) mixtures (spectra not shown). When 50 mol % cholesterol is added to aqueous dispersions of (14:0)(per-^2H-14:0)PC containing perdeuterated acyl chains in the *sn*-2 position alone, only one doublet is observed (spectra not shown), further substantiating the assignment of the two doublets to the two acyl chain methyl deuterons.

Order Parameter Profiles for di(per-^2H-14:0)PC. The overlapping powder patterns in the perdeuterated samples arise from the different average segmental orientations for the 12 individual methylene segments and the terminal methyl segment per acyl chain. The cumulative effect of trans–gauche configurational isomerism leads to the characteristic flexibility gradient of lipid bilayers, which is illustrated in Figure 2.

In addition to the order parameter profiles for bilayers formed from di(per-^2H-14:0)PC alone, the profiles for 3:1, 2:1, and 1:1 (mol/mol) mixtures of cholesterol with di(per-^2H-14:0)PC are shown in Figure 2. As can be seen from this figure, the general effect of addition of cholesterol to di(per-^2H-14:0)PC bilayers is to increase the S_{mol} values for all

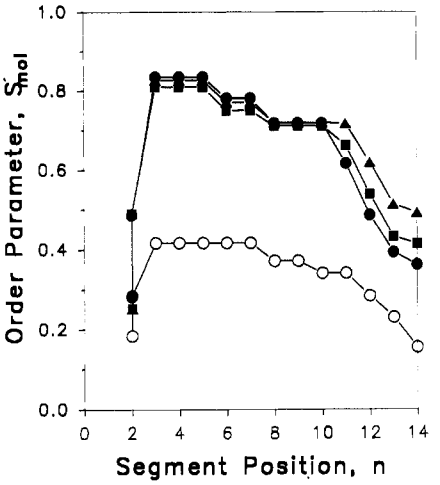

FIGURE 2: Cholesterol-induced changes in the segmental order parameter (S_{mol}) profiles of the *sn*-2 chain of di(per-^2H-14:0)PC in the l_o phase at 35 °C at a 3:1 (▲), 2:1 (■), and 1:1 (●) mole ratios of phospholipid to cholesterol and of di(per-^2H-14:0)PC alone (○).

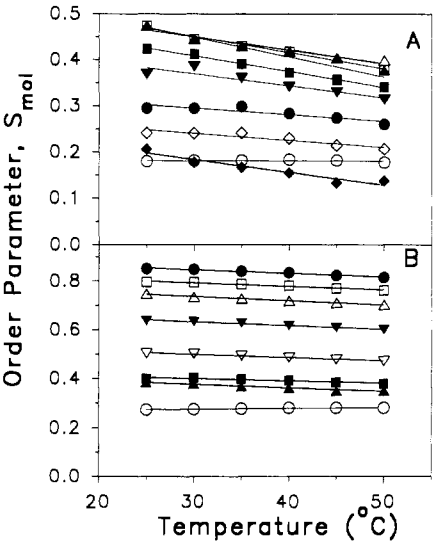

FIGURE 3: Temperature dependence of the segmental order parameters (S_{mol}) for aqueous dispersions of di(per-^2H-14:0)PC alone (A) and for an equimolar mixture of cholesterol with di(per-^2H-14:0)PC (B). The assignments of the S_{mol} values to the acyl chain carbon positions, *n*, of the *sn*-2 chain for the pure phospholipid system are n = 2 (○); n = 2′, 12 (●); n = 3, 4, 5 (△); n = 6 (▲); n = 7 (□); n = 8, 9 (■); n = 10 (▽); n = 11 (▼); n = 13 (◇); and n = 14 (◆). The assignments for the phospholipid–cholesterol mixture are n = 2 (○); n = 2′, 12 (▽); n = 3, 4, 5 (●); n = 6, 7 (□); n = 8, 9, 10 (△); n = 11 (▼); n = 13 (■); and n = 14 (▲). 2 and 2′ correspond to the inequivalent deuterons of the methylene group directly connected to the carbonyl groups.

the chain segments but to still retain the flexibility gradient. Second, the S_{mol} values are never equal to the expected value of unity for the all-trans acyl chain configuration. This is true in the concentration range 0–50 mol % cholesterol in liquid-crystalline lipid bilayers. Third, no significant differences are seen in the S_{mol} values for segments 2–10 for the 3:1, 2:1, and 1:1 phospholipid–cholesterol (mol/mol) complexes. Fourth, for the three cholesterol concentrations studied, the S_{mol} values *decrease* in the order 3:1 > 2:1 > 1:1.

Temperature Dependence of S_{mol} for di(per-^2H-14:0)PC. The temperature dependence of the segmental order parameters for aqueous dispersions of di(per-^2H-14:0)PC alone and for an equimolar mixture of cholesterol with di(per-^2H-14:0)PC are shown in parts A and B of Figure 3, respectively. The segmental order parameters for the methylene and methyl segments in the *sn*-2 chain were calculated from the quadru-

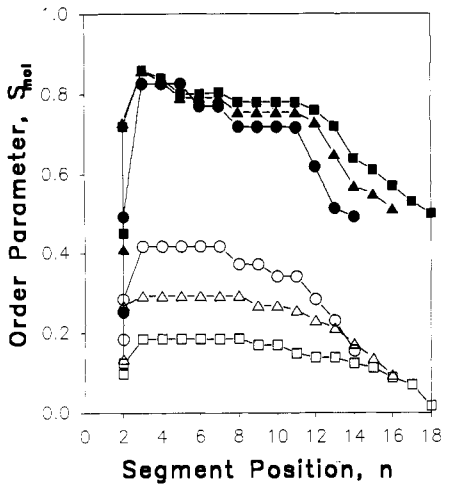

FIGURE 4: Segmental order parameter (S_{mol}) profiles of the *sn*-2 chain of di(per-^{2}H-14:0)PC (○, ●), di(per-^{2}H-16:0)PC (△, ▲), and di(per-^{2}H-18:0)PC (□, ■) in the presence (●, ▲, ■) and absence (○, △, □) of 50 mol % cholesterol. The data were obtained at 35 °C for di(per-^{2}H-14:0)PC, at 52 °C for di(per-^{2}H-16:0)PC, and at 63 °C for di(per-^{2}H-18:0)PC, corresponding to a constant reduced temperature of 0.041 ± 0.001.

pole splittings as described under Materials and Methods, taking into account the C_{3v} symmetry of the C^2H_3 group. The various quadrupole splittings seen in the spectra of di(per-^{2}H-14:0)PC were assigned to individual chain segments of the *sn*-1 and the *sn*-2 chains on the basis of earlier studies (Davis, 1979; Salmon et al., 1987) and by comparing the spectra with those of (14:0)(per-^{2}H-14:0)PC. Two interesting observations can be made by comparing the data in Figure 3A for the phospholipid alone with the data in Figure 3B for the equimolar cholesterol–phospholipid mixture. First, incorporation of 50 mol % cholesterol leads to a pronounced decrease in the temperature gradient of the S_{mol} values of the phospholipid acyl chains. The temperature coefficients of S_{mol} for the chain positions 3–13 range from -1.51×10^{-3}/°C to -4.3×10^{-3}/°C for the cholesterol-free di(per-^{2}H-14:0)PC dispersions. These values are reduced to the range of -1.23×10^{-3}/°C to -1.74×10^{-3}/°C for the equimolar mixture with cholesterol. Second, the ratio of S_{mol} values for any two positions is nearly independent of temperature in the cholesterol-containing system, while the ratios are strongly temperature-dependent for bilayers containing only phospholipid.

Order Parameter Profiles for di(per-^{2}H-14:0)PC, di(per-^{2}H-16:0)PC, and di(per-^{2}H-18:0)PC. The di(per-^{2}H-16:0)PC, (16:0)(per-^{2}H-16:0)PC, di(per-^{2}H-18:0)PC, and (18:0)(per-^{2}H-18:0)PC systems are similar in the following respect to the case of the di(per-^{2}H-14:0)PC and the (14:0)(per-^{2}H-14:0)PC systems described in detail above. First, the cholesterol-induced inequivalence of the *sn*-1 and *sn*-2 chain methyl group deuteron inequivalence is observed for both the di(per-^{2}H-16:0)PC and the di(per-^{2}H-18:0)PC systems and not for the (16:0)(per-^{2}H-16:0)PC and the (18:0)(per-^{2}H-18:0)PC systems. Second, the presence of cholesterol at an equimolar concentration alters the temperature dependence of the S_{mol} values for the three perdeuterated diacyl phosphatidylcholines in a manner very similar to that described above.

There are significant differences in the way the segmental order parameter profiles of the *sn*-2 chains of the di(per-^{2}H-14:0)PC, di(per-^{2}H-16:0)PC, and di(per-^{2}H-18:0)PC respond to the presence of an equimolar amount of cholesterol. The differences are illustrated in Figure 4, where the S_{mol} values for the *sn*-2 chains are plotted as a function of the chain segment position for the di(per-^{2}H-14:0)PC, di(per-^{2}H-16:0)PC, and di(per-^{2}H-18:0)PC bilayers in the presence and absence of an equimolar amount of cholesterol. The data are compared at a constant reduced temperature, $(T - T_c)/T_c$ of 0.041 ± 0.001, where T is the actual absolute temperature of measurement and T_c is the gel to liquid-crystalline phase transition temperature of the corresponding phospholipid bilayers without cholesterol.

When the order parameter profiles are compared at the same absolute temperature in the absence of cholesterol, the plateau region extends over a shorter range as the number of chain methylenes decreases. At a constant reduced temperature, the segmental order parameters decrease with increasing number of chain carbons, whereas at the same absolute temperature the opposite correlation is found.

As seen in Figure 4, the presence of an equimolar amount of cholesterol leads to an obliteration of the differences in the length of the plateau region and of the differences in the S_{mol} values at the same reduced temperature. For positions from 12 to the terminal methyl group, the cholesterol-induced increase in S_{mol} decreases in the order di(per-^{2}H-18:0)PC > di(per-^{2}H-16:0)PC > di(per-^{2}H-14:0)PC.

Discussion

Acyl Chain Order and Conformation in the l_o Phase. Most of the earlier ^{2}H NMR studies on binary mixtures of cholesterol with glycerophospholipids, using the perdeuterated stearic acid probe in egg yolk phosphatidylcholine (Stockton & Smith, 1976), di(per-^{2}H-16:0)PC (Vist & Davis, 1990), di(2-C^2H_2-16:0)PC (Haberkorn et al., 1977) and di(14:0)PC specifically deuterated at various positions in the *sn*-2 chain (Oldfield et al., 1978), were done at cholesterol concentrations between 0 and 30 mol %. These studies have shown that the effect of cholesterol is to increase the S_{mol} values for all the acyl chain positions at temperatures higher than the main-chain melting temperatures.

We now report studies with cholesterol concentrations up to 50 mol % in di(per-^{2}H-14:0)PC, di(per-^{2}H-16:0)PC, and di(per-^{2}H-18:0)PC bilayers. The data in Figure 2 for the di(per-^{2}H-14:0)PC–cholesterol system, and the data not shown for the di(per-^{2}H-16:0)PC– and di(per-^{2}H-18:0)PC–cholesterol systems, indicate that the S_{mol} values continue to decrease with increasing cholesterol concentration in this range. This behavior is reminiscent of the triphasic dependence of the hyperfine splitting constants of spin-labeled phospholipids on cholesterol concentration observed for phosphatidylcholines and sphingomyelin (Sankaram & Thompson, 1990). Oldfield et al. (1978) have reported that the quadrupole splittings of the headgroup choline methyl deuterons in the di(16:0)PC–cholesterol system reach a maximum between 20 and 25 mol % cholesterol and decrease with further increase in cholesterol concentration. They attribute this effect to a decrease in the crowding of the headgroups caused by a decrease in the density of the phosphatidylcholine molecules in the plane of the membrane. The decrease in S_{mol} values for segments beyond the 12th carbon is likely to occur by a similar mechanism. Defects in packing of the dissimilar phospholipid cholesterol molecules can contribute to this effect as well.

The temperature dependence of S_{mol} values of the di(per-^{2}H-14:0)PC shown in Figure 3 and of the di(per-^{2}H-16:0)PC and the di(per-^{2}H-18:0)PC systems reveals an interesting feature of the cholesterol-induced increase in the phospholipid acyl chain order. The straight lines drawn in this figure, depicting the linear dependence of S_{mol} on temperature, are rendered nearly parallel by cholesterol. This result can be interpreted in the following way. For a rigid molecule simply undergoing rapid axially symmetric reorientation about a single

Table I: Effective Acyl Chain Length from Carbonyl Carbon to Terminal Methyl Carbon Averaged for the *sn*-1 and the *sn*-2 Chains[a] Calculated from the Segmental Order Parameters (S_{mol}) for di(per-^{2}H-14:0)PC, di(per-^{2}H-16:0)PC, and di(per-^{2}H-18:0)PC Bilayers, Denoted 14:0, 16:0, and 18:0, Respectively, in the Absence and Presence of 3, 2, and 1 mol of Phospholipid Per Mole of Cholesterol[b]

phospho-lipid	1:0 (Å)	3:1 (Å)	2:1 (Å)	1:1 (Å)	all trans (Å)	T (°C)
di(14:0)PC	10.7	13.1	12.8	12.8	16.25	35
di(16:0)PC	11.6	15.3	14.9	14.5	18.75	52
di(18:0)PC	12.6	15.7	15.3	15.1	21.25	63

[a] The estimated accuracy in the chain lengths is ±0.2 Å. [b] The data are obtained at a constant reduced temperature of 0.041 ± 0.001.

axis, the segmental order parameters would be independent of temperature so long as the motion was rapid on the ^{2}H NMR time scale. If, however, the orientation of this symmetry axis fluctuates with respect to the direction of the external magnetic field, then all of the splittings of this rigid molecule will be reduced by the same relative amount. Internal motions such as those due to acyl chain configurational isomerism lead to a differential reduction of the quadrupole splittings for various chain segments. This simple model predicts that the ratio of any two of the segmental order parameters will be independent of temperature in the absence of internal motions even though the order parameters themselves may decrease as the temperature is raised (Davis, 1988). The data in Figure 3A for pure di(per-^{2}H-14:0)PC in aqueous dispersion clearly show that the ratios of segmented order parameters are not independent of temperature. Similar results are obtained for di(per-^{2}H-16:0)PC and di(per-^{2}H-18:0)PC (data not shown). However, upon addition of cholesterol to give an equimolar mixture as shown in Figure 3B the ratio of any pair of S_{mol} values is nearly invariant with temperature in the interval between segment 3 and the methylene segment next to the terminal methyl group. This indicates that the amplitudes of internal motions of the phospholipid molecules in this system are substantially reduced.

Effective Acyl Chain Lengths in Perdeuterated, Saturated Diacylphosphatidylcholines. The S_{mol} values for the di(per-^{2}H-14:0)PC–, di(per-^{2}H-16:0)PC–, and di(per-^{2}H-18:0)PC–cholesterol systems can be used to calculate the effective lengths of the *sn*-1 and *sn*-2 chains of the phospholipids at various mole fractions of cholesterol. Table I gives the effective chain lengths averaged for the *sn*-1 and the *sn*-2 chains, from the carbonyl carbon to the terminal methyl carbon, calculated according to the method of Seelig and Seelig (1974). The ^{2}H NMR data used in this analysis are obtained from perdeuterated phospholipids. As a result, the resolution of the various Pake doublets is limited and the spectral assignments tend to become uncertain when the plateau region extends over a longer carbon atom span. This uncertainty leads to an underestimate of the effective chain length. Phospholipids deuterated at specific chain segments provide more accurate data (Sankaram & Marsh, 1989). At 52 °C we obtain a value of 11.6 Å for di(per-^{2}H-16:0)PC, as shown in Table I. This is in good agreement with a value of 13.15 Å at 50 °C calculated for the *sn*-2 chain of di(16:0)PC by Seelig and Seelig (1974) using specifically deuterated phospholipids. In their calculation, Seelig and Seelig (1974) used interpolated S_{mol} values for six of the 15 segments. Examination of the effective chain lengths for the three phosphatidylcholines when cholesterol is present shows that the chain lengths increase but not to the all-trans values listed in the sixth column of Table I. Although the differences are small, it also appears that, for a given phosphatidylcholine, the effective chain length is greatest for the lowest cholesterol concentration (25 mol %).

It is interesting to compare the chain length data determined from ^{2}H NMR order parameters with the length of the cholesterol molecule. The average distance from the carbonyl carbon in the acyl chain to the terminal methyl carbon in Table I ranges from 12.8 to 15.7 Å for the various mixtures of cholesterol with the three different phosphatidylcholines. This distance is substantially shorter than the 20-Å length of the cholesterol molecule determined from the crystal structure, which includes both the rigid part and an extended conformation for the side chain [Craven, 1976; see Huang (1977) and Yeagle (1988)]. The side chain of cholesterol has some degree of flexibility as seen both in its various polymorphic crystalline forms (Shieh et al., 1981) and in conformational studies (Duax et al., 1988). This conformational flexibility of the side chain leads to an uncertainty of ±2 Å in the length of the cholesterol molecule.

It has been suggested that cholesterol is anchored in the bilayer by a hydrogen bond between its hydroxyl group and the *sn*-2 carbonyl [Huang, 1976; Huang & Mason, 1982; see Yeagle (1988)]. If this is the case, part of the cholesterol molecule in one monolayer must extend into the other monolayer to compensate for the mismatch between cholesterol and acyl chain lengths. Such an arrangement is analogous to the packing modes in interdigitated one- and two-component phospholipid bilayers where the acyl chain ends do not meet at the center of the bilayer (Slater & Huang, 1988; Huang, 1990). An alternative arrangement would be a hydrogen bond between cholesterol and the phosphate moiety of the phosphatidylcholine headgroup. The average distance from the phosphate group to the terminal methyl should then be compared with the length of the cholesterol molecule. The phosphate to methyl group distances can be obtained from the chain lengths determined from the S_{mol} values by adding a constant distance of 6.25 Å for the carbonyl to the phosphate group, projected onto the long axis of the lipid bilayer, estimated from the crystal structure of di(14:0)PC (Pearson & Pascher, 1979). In this case, the phosphate–methyl group distances range from 19.3 to 22.2 Å, calculated from the data in Table I. Since these values are close to the length of the cholesterol molecule, the methyl group terminals of the phospholipid and the cholesterol molecules will be in register at the midplane of the bilayer.

Calculation of Bilayer Thickness. The acyl chain lengths given in Table I can be used to obtain the expected bilayer thickness or the transbilayer interphosphate distance. For the pure phosphatidylcholines, bilayer thickness can be calculated by using the following equation:

$$d_0 = 2\,[L_{P\text{-}2} + L^0 + L_{C\text{-}H}] + L_{H\cdots H} \qquad (4)$$

In this equation, $L_{P\text{-}2}$ is the distance from the phosphorus atom in the headgroup to the second carbon atom in the acyl chain projected onto the long axis, L^0 is the chain length calculated from the ^{2}H NMR determined S_{mol} values, $L_{C\text{-}H}$ is the carbon–hydrogen single-bond length to account for the terminal methyl group, and $L_{H\cdots H}$ is the hydrogen–hydrogen van der Waals radius. $L_{C\text{-}H}$ and $L_{H\cdots H}$ are 1.09 and 1.0 Å, respectively (Handbook of Physics and Chemistry, 1988). $L_{P\text{-}2}$ is estimated to be 6.25 Å from the crystal structure of di(14:0)PC (Pearson & Pascher, 1979). From the values of L^0 in Table I, the bilayer thicknesses calculated for di(per-^{2}H-14:0)PC, di(per-^{2}H-16:0)PC, and di(per-^{2}H-18:0)PC are 37 Å (35 °C), 38.8 Å (52 °C), and 40.8 Å (63 °C), respectively. The electron density profiles for di(14:0)PC, di(16:0)PC, and di(18:0)PC yield interphosphate distances of 34 Å (36 °C), 37 Å (44 °C), and 40.5 Å (60 °C), respectively [see Lewis

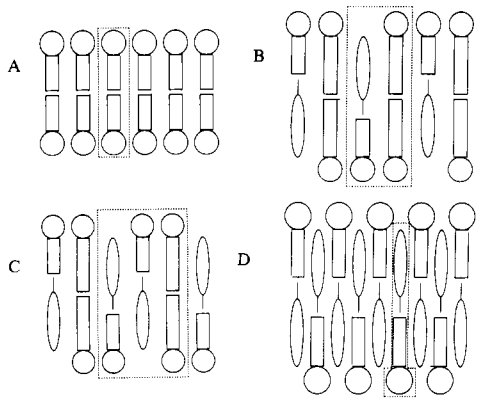

FIGURE 5: Characteristic arrangements used for calculating the bilayer thickness for homogeneous mixtures of (A) the phospholipid alone and (B) 3:1, (C) 2:1, and (D) 1:1 phospholipid–cholesterol (mol/mol). These diagrams are not static packing arrangements of the component molecules but rather approximations of the time-averaged arrangements of them in the bilayer. The rigid four-ring moiety and the flexible end of the cholesterol molecule are represented by an ellipse and a line, respectively. The acyl chains of the phospholipids are illustrated by rectangular boxes and the hydrophilic region is shown as circles. For each system, the repeating units are enclosed in dashed rectangular boxes.

& Engelman (1983)]. By use of the linear thermal expansion coefficient for phospholipid bilayers of -3.0×10^{-3}/°C (Luzzati & Husson, 1962) determined by X-ray diffraction experiments, the experimental thickness data can be extrapolated to the temperatures where the thickness was determined from ^{2}H NMR methods. Thus scaled, the phosphate peak spacings are 33 Å for di(14:0)PC at 35 °C, 36.2 Å for di(16:0)PC at 52 °C, and 40.2 Å for di(18:0)PC at 63 °C, which are in good agreement with the ^{2}H NMR determined interphosphate distances. For these calculations, any possible acyl chain tilting with respect to the bilayer normal is not taken into consideration. This factor would reduce the calculated interphosphate distances by about 4.1 Å for a tilt angle of 27° [see Seelig and Seelig (1974)].

In order to extend the calculation of bilayer thickness to the phosphatidylcholine/cholesterol bilayers certain assumptions are necessary. First, in accord with phase diagram information for di(16:0)PC, let us assume for all systems that no microscopic lateral phase separation occurs in the cholesterol concentration interval 25–50 mol %. Second, let us assume in a time-averaged, statistical sense that the many possible arrangements of cholesterol and phosphatidylcholine molecules can be represented by a single, characteristic arrangement that is unique for each cholesterol concentration. This characteristic arrangement is not intended to represent a complex but rather an approximation of the time-averaged arrangements of the molecules in the bilayer. It affords a basis for calculating bilayer thickness values to a reasonable approximation. The possible ways of arranging the phospholipid and cholesterol molecules to achieve a characteristic time-averaged model at different mole ratios are shown in Figure 5. Aqueous dispersions formed from the phospholipids alone can be described by a repeating unit consisting of two phospholipid molecules (Figure 5A). In the case of the equimolar mixture, a bilayer consisting of a single phospholipid molecule and a single cholesterol molecule can be treated as a repeating unit to form a homogeneous mixture as shown in Figure 5D. The bilayer thickness for an equimolar mixture, $d_{1:1}$, is then given by

$$d_{1:1} = L_{p-2} + L^{1:1} + L_{C-H} + L_{H\cdots H} + L_{Chol} \quad (5)$$

where $L^{1:1}$ is the effective acyl chain length obtained from the segmental order parameters for the equimolar mixture and L_{Chol} is the length of the cholesterol molecule.

Table II: Average Bilayer Thickness[a] (Å) Obtained from the Segmental Order Parameters (S_{mol}) for Bilayers Formed from di(per-^{2}H-14:0)PC, di(per-^{2}H-16:0)PC, and di(per-^{2}H-18:0)PC Alone and from 3:1, 2:1, and 1:1 Molar Mixtures of Them with Cholesterol[b]

phospholipid	1:0 (Å)	3:1 (Å)	2:1 (Å)	1:1 (Å)
di(14:0)PC	37.0	41.6	41.1	41.1
di(16:0)PC	38.9	44.9	43.9	42.8
di(18:0)PC	40.8	46.9	44.5	43.4

[a] The bilayer thickness values are accurate to ±2 Å. [b] The temperatures are 35, 52, and 63 °C for di(14:0)PC, di(16:0)PC, and di(18:0)PC, respectively, and correspond to a constant reduced temperature of 0.041 ± 0.001.

The repeating unit for the 3:1 mixture (Figure 5B) consists of three phospholipid molecules and one cholesterol. This repeating unit is obtained by placing the repeating units for the cholesterol-free (Figure 5A) and the equimolar cholesterol–phospholipid systems (Figure 5D) parallel to each other. The phospholipid molecules in the transbilayer cholesterol–phospholipid pairs have a shorter acyl chain length than those in the phospholipid–phospholipid pairs. Therefore, the effective acyl chain lengths determined from the S_{mol} values are weighted averages of the chain lengths of the shorter and the longer phospholipid molecules. Assuming that the chain length of the shorter molecules is $L^{1:1}$, the value determined for the equimolar mixture, the acyl chain length for the longer phospholipid molecules in the 3:1 mixture is given by $(3L^{3:1} - L^{1:1})/2$. The bilayer thickness for this mixture is then given by

$$d_{3:1} = (1/2)[d_0 + d_{1:1}] \quad (6)$$

where d_0 is calculated according to eq 4 by using $(3L^{1:1} - L_{1:1})/2$ as the acyl chain length.

The 2:1 phospholipid–cholesterol mixture could be described as an infinite repeat of a unit containing four phospholipid molecules and two cholesterol molecules (Figure 5C). This repeating unit is obtained by a lateral juxtaposition of the repeating unit for the 1:1 complex (Figure 5D) and the repeating unit for the 3:1 complex (Figure 5B). The effective chain lengths of the shorter and the longer phospholipid molecules can be calculated again from the experimentally determined average acyl chain lengths for a 2:1 mixture, $L^{2:1}$ as outlined above for the 3:1 mixture. As before, when the shorter acyl chain length is assumed to be $L^{1:1}$, the longer chain length is given by $(2L^{2:1} - L^{1:1})$. For this configuration, the bilayer thickness is given by

$$d_{2:1} = (1/3)[d_0 + 2d_{1:1}] \quad (7)$$

where d_0 is determined from eq 4, but by using the longer acyl chain length.

In general, for any mole ratio of phospholipid to cholesterol, the bilayer thickness can be operationally defined in terms of the thickness contribution from phospholipid–phospholipid pairs, d_0, and from phospholipid–cholesterol pairs, $d_{1:1}$. If the mole ratio of phospholipid to cholesterol is n:1, then the effective bilayer thickness, $d_{n:1}$, is given by

$$d_{n:1} = 1/(n+1)[(n-1)d_0 + 2d_{1:1}] \quad (8)$$

where d_0 is calculated by using eq 4 with $(nL - L^{1:1})/(n-1)$ as L^0 and $d_{1:1}$ is given by eq 5.

Table II gives the bilayer thickness calculated by eqs 5–7 from the ^{2}H NMR determined effective chain lengths $L^{1:1}$, $L^{2:1}$, and $L^{3:1}$ listed in Table I. At a constant reduced temperature of, for example, 0.041, the bilayer thickness values obtained for the various mixtures with cholesterol lie in the range 41.1–46.9 Å. With increasing cholesterol concentration in the

3:1 to 1:1 mole ratio range, the bilayer thickness decreases for all the three phospholipid–cholesterol systems. This is to be expected from data shown in Figure 3, where the S_{mol} values decrease with increasing cholesterol concentration for part of the chain segments. Also, in terms of the models in Figure 5 used for the calculation of the bilayer thickness, the proportion of the 1:1 transbilayer phospholipid–cholesterol pairs increases with increasing cholesterol concentration. Since the phospholipids involved in this pairing are shorter than those involved in the transbilayer phospholipid–phospholipid pairing, the bilayer thickness must decrease with increasing cholesterol concentration. This is true even if the effective weighted-average chain length determined from the S_{mol} values remains constant as a function of cholesterol concentration.

Electron density profiles constructed at 20 °C for di(16:0)PC–cholesterol and di(18:0)PC–cholesterol mixtures at a 2:1 phospholipid–cholesterol mole ratio (McIntosh, 1978) give a bilayer thickness of 46 Å for the di(16:0)PC–cholesterol mixture and 50 Å for di(18:0)PC–cholesterol. The transbilayer interphosphate distances calculated for the model shown in Figure 5C, where the cholesterol hydroxyl group is placed adjacent to the phospholipid *sn*-2 carbonyl, from S_{mol} data at 20 °C for 2:1 mixtures (data not shown) are 46 Å for the di(per-^{2}H-16:0)PC–cholesterol system and 48 Å for the di(per-^{2}H-18:0)PC–cholesterol system. The bilayer thickness determined from the same S_{mol} data but by placing the cholesterol hydroxyl next to the phosphate group is shorter by 4 Å. Our data are, therefore, consistent with a hydrogen bond between the hydroxyl group of cholesterol and the *sn*-2 carbonyl of the phospholipid molecule.

Ipsen et al. (1990) have proposed a comprehensive microscopic interaction model that establishes interrelationships between order parameters, membrane hydrophobic thickness, and membrane area. One noteworthy difference between this model and the one presented in this paper is in the definition of the membrane thickness and the way the order parameters are obtained from the ^{2}H NMR spectra. The membrane thickness in our model is given by eq 8 and can be compared to thickness values obtained from independent experimental studies such as electron density profiles. The hydrophobic thickness used by Ipsen et al. (1990) covers approximately the transbilayer intercarbonyl distance, which is difficult to obtain from other direct measurements of membrane thickness.

The High Cholesterol Concentration l_o Phase. Both the acyl chain lengths obtained from the S_{mol} values and the bilayer thickness calculated by using the models shown in Figure 5 suggest a partial interdigitation of cholesterol in the l_o phase, which arises from a molecular length mismatch. The packing arrangement in the l_o phase for an equimolar mixture is shown in Figure 6A. It is important to note that even in the absence of trans–gauche configurational isomerism, the all-trans chains of di(14:0)PC, di(16:0)PC, and di(18:0)PC are shorter than the length of cholesterol molecule as shown in Table I.

The l_o phase is characterized by a rapid axially symmetric motion (Cornell & Keniry, 1983; van Ginkle et al., 1986; Vist & Davis, 1990) and fast lateral diffusion (Rubenstein et al., 1979; Alecio et al., 1982) typical of phospholipids in bilayers above the gel to liquid-crystalline phase transition temperatures. Yet, the orientational order and the spectral moments are much higher than those for pure phospholipid bilayers in the liquid-crystalline state (see Figure 4; Stockton & Smith, 1976; Haberkorn et al., 1977; Oldfield et al., 1978; Jacobs & Oldfield, 1979; Recktenwald & McConnell, 1981; Presti & Chan, 1982; Wolber & Hudson, 1981; Kutchai et al., 1983; Vist & Davis, 1990) and are comparable to values in the gel

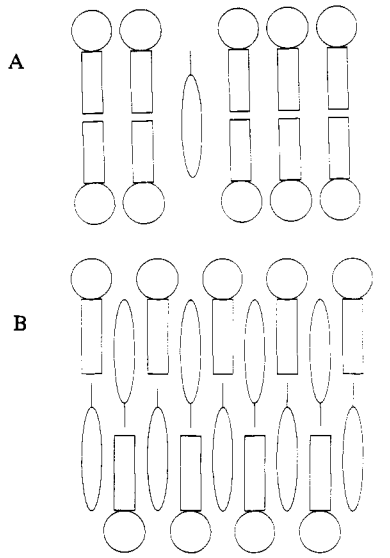

FIGURE 6: Characteristic time-averaged arrangements for (A) the liquid-ordered (l_o) phase at a 1:1 phospholipid–cholesterol mole ratio and (B) the liquid-disordered (l_d) phase of phospholipid–cholesterol mixtures.

phase. The area compressibility modulus for the l_o phase of di(14:0)PC–cholesterol mixtures (Needham et al., 1988) is close to the value obtained for the gel phase of di(14:0)PC.

The Low Cholesterol Concentration l_d Phase. The data in Table I indicate that the transbilayer carbonyl–carbonyl distance is between 24 and 28 Å for di(per-^{2}H-14:0)PC, di(per-^{2}H-16:0)PC, and di(per-^{2}H-18:0)PC. The ^{2}H NMR data of Vist and Davis (1990) in the l_d phase correspond to much shorter acyl chains than the l_o phase studied here (see later). The carbonyl–carbonyl distances in the l_d phase estimated from the data of Vist and Davis (1990) do not change appreciably in the cholesterol concentration range 0–10 mol %. Small-angle X-ray diffraction results (Hui & He, 1983) show that the repeat spacings remain unchanged when 5 mol % cholesterol is added to di(14:0)PC bilayers at temperatures higher than 23 °C. These data suggest that the acyl chains do not become significantly longer in the l_d phase and that the average transbilayer intercarbonyl distances are between 20 and 30 Å. Therefore, the cholesterol molecule can be accommodated in phospholipid bilayers in the l_d phase spanning the entire hydrophobic core of the bilayer. This model, shown schematically in Figure 6B, predicts that the phase boundary between the l_d phase and $l_d - l_o$ coexistence phase line occurs at smaller cholesterol concentrations as the number of methylenes in the acyl chains is increased. Indeed, the partial phase diagrams constructed for binary mixtures of cholesterol with di(14:0)PC, di(16:0)PC, and di(18:0)PC do bear this out (Sankaram & Thompson, 1990). In addition, it has been found that this boundary is shifted to higher cholesterol concentrations as the temperature is increased (Ipsen et al., 1987; Sankaram & Thompson, 1990). Since the acyl chains of the phospholipids are shorter at higher temperatures due to increased trans–gauche isomerism, this experimental observation is consistent with the model proposed for the l_d phase. The chains become considerably longer as the concentration of cholesterol is increased beyond the low cholesterol concentration phase boundary line when the hydrophobic core of the phospholipid bilayers can no longer accommodate a cholesterol molecule in this configuration. The system then begins to form the l_o phase. As long as the transbilayer intercarbonyl distance is much shorter than the added length of two cholesterol molecules, part of the cholesterol molecule in one monolayer

extends into the other monolayer. This model with a transbilayer arrangement of cholesterol at one extreme of the temperature–composition phase diagram (in the l_d phase) and a partially interdigitated phospholipid–cholesterol mixture at the other extreme (l_o phase) provides a molecular basis for fluid–fluid immiscibility in phospholipid bilayers induced by cholesterol. Further NMR evidence for these two models will be presented in another publication.

The models in Figure 5 for the various phospholipid–cholesterol mixtures and those in Figure 6 for the l_d and the l_o phases differ in a fundamental way from those proposed earlier in the literature. Previous interpretations of the binary phase diagrams of cholesterol-containing phospholipid bilayers and of the spectral and calorimetric behavior have involved the formation of specific 4:1, 3:1, 2:1, or 1:1 stoichiometric complex formation between cholesterol and phospholipids (see Introduction). The model we propose does not require complex formation. Rather the models, shown in Figure 5, are time-averaged arrangements of cholesterol and phosphatidylcholines characteristic of the various mixtures. The fluid phase immiscibility is thus suggested to be a natural consequence of, and modulated by, the acyl chain length mismatch between the flexible phospholipid molecules with the rigid cholesterol molecules where the phospholipid acyl chain length itself is affected by the presence of varying amounts of cholesterol.

ACKNOWLEDGMENTS

We thank Dr. Zhao-Qing Wang for the synthesis of the deuterated phospholipids and Dr. Hai-nan Lin for help with the differential scanning calorimeter. We would like to acknowledge the many inspiring discussions with Dr. Ching-hsien Huang, particularly his comments on the deuterium-isotope effect. We thank Drs. Yechezkel Barenholz, Rodney Biltonen, and Ching-hsien Huang for critically reading the manuscript. We are grateful to Drs. M. Bloom, E. Sternin, and K. Whittall of the University of British Columbia for their noniterative and iterative de-Pakeing programs.

Registry No. Di(14:0)PC, 18194-24-6; di(16:0)PC, 63-89-8; di(18:0)PC, 816-94-4; cholesterol, 57-88-5.

REFERENCES

Alecio, M. R., Golan, D. E., Veatch, W. R., & Rando, R. R. (1982) *Proc. Natl. Acad. Sci. U.S.A. 79*, 5171–5174.

Bloom, M., Davis, J. H., & Valic, M. I. (1980) *Can. J. Phys. 58*, 1510–1517.

Bloom, M., Davis, J. H., & MacKay, A. L. (1981) *Chem. Phys. Lett. 80*, 198–202.

Boesze-Battaglia, K., Hennessey, T., & Albert, A. D. (1989) *J. Biol. Chem. 264*, 8151–8155.

Burnett, L. J., & Muller, B. H. (1971) *J. Chem. Phys. 55*, 5829–5839.

Cooper, R. A. (1977) *N. Engl. J. Med. 297*, 371–377.

Copeland, B. R., & McConnell, H. M. (1980) *Biochim. Biophys. Acta 599*, 95–109.

Cornell, B. A., & Keniry, M. (1983) *Biochim. Biophys. Acta 732*, 705–710.

Craven, B. M. (1976) *Nature (London) 260*, 727–729.

Davis, J. H. (1979) *Biophys. J. 27*, 339–358.

Davis, J. H. (1983) *Biochim. Biophys. Acta 737*, 117–171.

Davis, J. H. (1988) *Biochemistry 27*, 428–436.

Davis, J. H., Jeffrey, K. R., Bloom, M., Valic, M. I., & Higgs, T. P. (1976) *Chem. Phys. Lett. 42*, 390–394.

Davis, J. H., Bloom, M., Butler, K. W., & Smith, I. C. P. (1980) *Biochim. Biophys. Acta 597*, 447–491.

Duax, W. L., Wawrzak, Z., Griffin, J. F., & Cheer, C. (1988) in *The Biology of Cholesterol* (Yeagle, P. L., Ed.) pp 1–18, CRC Press Inc., Boca Raton, FL.

Engelman, D. M., & Rothman, J. E. (1972) *J. Biol. Chem. 247*, 3694–3697.

Estep, T. N., Mountcastle, D. B., Biltonen, R. L., & Thompson, T. E. (1978) *Biochemistry 17*, 1984–1989.

Haberkorn, R. A., Griffin, R. G., Meadows, M. D., & Oldfield, E. (1977) *J. Am. Chem. Soc. 99*, 7353–7355.

Handbook of Chemistry and Physics (1988) CRC Press, Boca Raton, FL.

Hinz, H. J., & Sturtevant, J. M. (1972) *J. Biol. Chem. 247*, 3697–3700.

Huang, C.-H. (1976) *Nature (London) 259*, 242–243.

Huang, C.-H. (1977) *Lipids 4*, 348–356.

Huang, C.-H. (1990) *Klin. Wochenschr. 68*, 149–165.

Hui, S. W., & He, N.-B. (1983) *Biochemistry 22*, 1159–1164.

Ipsen, J. H., Karlström, G., Wennerström, & Zuckermann, M. J. (1987) *Biochim. Biophys. Acta 905*, 162–172.

Jacobs, R., & Oldfield, E. (1979) *Biochemistry 18*, 3280–3285.

Kleemann, W., & McConnell, H. M. (1976) *Biochim. Biophys. Acta 419*, 206–222.

Kutchai, H., Chandler, L. H., & Zavoico, G. B. (1983) *Biochim. Biophys. Acta 736*, 137–149.

Lecuyer, H., & Dervichian, D. G. (1969) *J. Mol. Biol. 45*, 39–57.

Lentz, B. R., Barrow, D. A., & Hoechli, M. (1980) *Biochemistry 19*, 1943–1954.

Lewis, B. A., & Engelman, D. M. (1983) *J. Mol. Biol. 166*, 211–217.

Luzzati, V., & Husson, F. (1962) *J. Cell Biol. 12*, 207–214.

Mabrey, S., Mateo, P. L., & Sturtevant, J. M. (1978) *Biochemistry 17*, 2464–2468.

Mason, J. T., Broccoli, A. V., & Huang, C. (1981) *Anal. Biochem. 113*, 96–101.

McIntosh, T. J. (1978) *Biochim. Biophys. Acta 513*, 43–58.

Melchior, D. L., Scavitto, F. J., & Steim, J. M. (1980) *Biochemistry 19*, 4828–4834.

Needham, D., McIntosh, T. J., & Evans, E. (1988) *Biochemistry 27*, 4668–4673.

Oldfield, E., Meadows, M., Rice, D., & Jacobs, R. (1978) *Biochemistry 17*, 2727–2740.

Opella, S. J., Yesinowski, J. P., & Waugh, J. S. (1976) *Proc. Natl. Acad. Sci. U.S.A. 73*, 3812–3815.

Pearson, R. H., & Pascher, I. (1979) *Nature (London) 281*, 499–501.

Phillips, M. C., & Finer, E. G. (1974) *Biochim. Biophys. Acta 356*, 199–203.

Presti, F. T., & Chan, S. I. (1982) *Biochemistry 21*, 3821–3830.

Rance, M., Jeffrey, K. R., Tulloch, A. P., Butler, K. W., & Smith, I. C. P. (1982) *Biochim. Biophys. Acta 688*, 101–200.

Recktenwald, D. J., & McConnell, H. M. (1981) *Biochemistry 20*, 4505–4510.

Rouser, G., Nelson, G. J., Fleischer, S., & Simon, G. (1968) in *Biological Membranes* (Chapman, D., Ed.) pp 5–69, Academic Press, London.

Rubenstein, J. L. R., Smith, B. A., & McConnell, H. M. (1979) *Proc. Natl. Acad. Sci. U.S.A. 76*, 15–18.

Salmon, A., Dodd, S. W., Williams, G. D., Beach, J. M., & Brown, M. F. (1987) *J. Am. Chem. Soc. 109*, 2600–2609.

Sankaram, M. B., & Marsh, D. (1989) *Biophys. J. 56*, 1043–1044.

Sankaram, M. B., & Thompson, T. E. (1990) *Biochemistry* (preceding paper in this issue).

Seelig, A. (1977) *Q. Rev. Biophys. 10*, 353–418.

Seelig, A., & Seelig, J. (1974) *Biochemistry 13*, 4839–4845.
Seelig, A., & Seelig, J. (1980) *Q. Rev. Biophys. 13*, 19–61.
Shieh, H.-S., Hoard, L. G., & Nordman, C. E. (1981) *Acta Crystallogr. B37*, 1538–1543.
Shimshick, E. J., & McConnell, H. M. (1973) *Biochem. Biophys. Res. Commun. 53*, 446–451.
Slater, J. L., & Huang, C. H. (1988) *Prog. Lipid Res. 27*, 325–359.
Snyder, B., & Freire, E. (1980) *Proc. Natl. Acad. Sci. U.S.A. 77*, 4055–4059.
Sperotto, M. M., Ipsen, J. H., & Mouritsen, O. G. (1989) *Cell Biophys. 14*, 79–95.
Sternin, E., Bloom, M., & MacKay, A. L. (1983) *J. Magn. Reson. 55*, 274–282.
Stockton, G. W., & Smith, I. C. P. (1976) *Chem. Phys. Lipids 17*, 251–263.
Stockton, G. W., Polnaszek, C. F., Tulloch, A. P., Hasan, F., & Smith, I. C. P. (1976) *Biochemistry 15*, 954–966.
van Ginkle, G., Korstanje, L. J., van Langen, H., & Levine, Y. K. (1986) *Faraday Discuss. Chem. Soc. 81*, 49–61.
Vist, M. R., & Davis, J. H. (1990) *Biochemistry 29*, 451–464.
Whittall, K. P., Sternin, E., Bloom, M., & MacKay, A. L. (1989) *J. Magn. Reson. 84*, 64–71.
Wolber, P. K., & Hudson, B. S. (1981) *Biochemistry 20*, 2800–2810.
Yeagle, P. L. (1985) *Biochim. Biophys. Acta 822*, 267–287.
Yeagle, P. L. (1988) in *The Biology of Cholesterol* (Yeagle, P. L., Ed.) CRC Press Inc., Boca Raton, FL.

Evidence for a Direct Role for Sialic Acid in the Attachment of Encephalomyocarditis Virus to Human Erythrocytes†

Amir Tavakkol‡ and Alfred T. H. Burness*
Faculty of Medicine, Memorial University of Newfoundland, St. John's, Newfoundland, Canada A1B 3V6
Received May 1, 1990; Revised Manuscript Received August 14, 1990

ABSTRACT: Sialic acid residues are required in cellular receptors for many different mammalian viruses. Sialic acid could have a *direct role*, being an integral part of the virus binding site on the receptor. Alternatively, negatively charged sialic acid could have an *indirect role*, being responsible for holding the receptor in the required configuration for virus recognition, for instance, by interacting with positively charged amino acid residues found in the polypeptide chain of receptors. We have investigated the role of sialic acid in virus attachment by studying the interaction of the small RNA virus encephalomyocarditis (EMC) with glycophorin A, its receptor on human erythrocytes. In several experiments, influenza virus A was used for control purposes. Blocking positive charges on glycophorin either in lysine residues by acetylation or in arginine residues with butanedione did not affect its interaction with EMC virus. In contrast, blocking negatively charged carboxyl groups in sialic acid residues by amidation destroyed the ability of glycophorin to inhibit EMC virus attachment suggesting an important role for this part of sialic acid in EMC virus attachment. Removal of the polyhydroxy side chain in sialic acid residues of glycophorin by mild oxidation with periodate followed by reduction with borohydride had little effect on its interaction with EMC virus. Further, sialic acid species with either an acetyl or glycolyl group attached to the amino group on position 5 interacted equally well with EMC virus. We conclude that sialic acid residues play a direct role in attachment of EMC virus to its receptor forming part of the binding site itself, rather than the indirect role of interacting with basic amino acids to maintain the integrity of the attachment site on the receptor.

Many viruses such as influenza virus (Kathan et al., 1961; Marchesi & Andrews, 1971; Allaway & Burness, 1986), encephalomyocarditis (EMC)[1] virus (Enegren & Burness, 1977; Allaway & Burness, 1986), reovirus (Paul & Lee, 1987), and bluetongue virus (Eaton & Crameri, 1989) attach to human red cells by means of glycophorin A, which is the most abundant sialoglycoprotein in the human erythrocyte surface membrane (Furthmayr, 1978). Attachment of all four viruses is inhibited by pretreatment of red cells or glycophorin preparations with neuraminidase (sialidase), suggesting a role for sialic acid in the process.

Sialic acid could have one or two roles in virus attachment (Burness, 1981). It could have a direct role, being the moiety, or at least an important part of the site, to which these viruses bind. Alternatively, negatively charged sialic acid residues could have an indirect role, interacting with positively charged amino acids in glycophorin A holding the receptor in the appropriate three-dimensional configuration for virus binding. An indirect role for sialic acid would allow each virus to bind to its own specific region of glycophorin, but attachment of all would be inhibited by one enzyme, neuraminidase.

An indirect role for sialic acid in virus attachment leads to the prediction that blocking glycophorin A lysine ϵ-amino groups by acetylation or arginine guanidyl groups by butanedione should inhibit attachment of the receptor to viruses. We have tested these predictions in the study reported here. We show that neither treatment affected the interaction of

† Supported by grants from the Canadian Medical Research Council and the Canadian Diabetes Association.
* To whom correspondence should be addressed.
‡ Present address: Department of Dermatology, R6558, Kresge I, University of Michigan Medical School, Ann Arbor, MI 48109-0314.

[1] Abbreviations: EMC, encephalomyocarditis; PBS, phosphate-buffered saline; phosphate–NaCl, 0.1 M NaCl in 0.02 M phosphate buffer, pH 8.0.

0006-2960/90/0429-10684$02.50/0